International Journal of Bifurcation and Chaos

Logistic map with a first order filter

Risto Holopainen
Department of Musicology, University of Oslo, Norway
risto.holopainen@imv.uio.no

Received (to be inserted by publisher)

A lowpass filter inserted into the logistic map stabilizes fixed points of the system for large parameter ranges and increases the range of global stability. With a first order filter we get a special case of the general 2-D quadratic map with hyperchaos in parts of its parameter ranges. Filtered maps include some maps with delayed variables, and here we present one of the simplest examples of such a system.

Keywords: Logistic map; filtered maps; sound synthesis; transients; hyperchaos

1. Introduction

Apparently, nonlinear maps combined with linear time invariant filters in the feedback path have not been studied very much from a chaotic systems perspective. However, even a second-order digital filter implemented with 2's complement integer arithmetic may become chaotic when overflow occurs [Chua & Lin, 1988]. Here we consider only filters with floating point arithmetic.

A general formulation of this type of system, which we will call *filtered maps*, is

$$x_{n+1} = f(y_n) \tag{1}$$

$$y_n = \sum_{k=0}^{M} a_k x_{n-k} - \sum_{k=1}^{N} b_k y_{n-k} \tag{2}$$

where $f : \mathbb{R} \to \mathbb{R}$ is a nonlinear function, and $a_k, b_k \in \mathbb{R}$ are the filter coefficients. An even more general formulation would be to define filtered maps over the field of complex numbers. As defined here, filtered maps are autonomous systems, and the filters are always situated in the feedback path of the system. Strictly speaking, then, the filter in (1–2) is always recursive. Nevertheless, we retain standard filter terminology and refer to the filter as recursive only if it has at least one nonzero b coefficient.

Filtered maps arise, for example, in physical models of acoustic musical instruments [Rodet, 1993; Rodet & Vergez, 1999]. In that case the filter consists of a long delay, usually combined with lowpass and allpass filters. Delays of length D can be introduced by setting a_D in (2) to some nonzero value. The delay length, being the reciprocal of the fundamental frequency, can be adjusted to produce different pitches. Not only periodic sounds, but also chaotic vibrations are known to occur in woodwind multiphonics [Bernardi *et al.*, 1997]. Thus any realistic physical model of a woodwind instrument will be capable of producing both periodic and chaotic orbits. Filtered maps are also useful for a better understanding of other feedback-based sound synthesis algorithms [Holopainen, 2010].

Although filtered maps cover many kinds of systems, not all maps with delayed variables are instances of the system (1–2). For example, Buchner & Żebrowski [2000] studied a logistic map with delayed feedback, which at a casual glance looks similar to the system we will shortly introduce, although their delayed logistic map cannot be transformed into a filtered map.

One of the simplest examples of a filtered map is obtained by taking the logistic map in the form $f(x) = rx(1-x), r \in \mathbb{R}$, and combining it with a first order nonrecursive filter into the system

$$x_{n+1} = ry_n(1-y_n) \tag{3}$$
$$y_n = ax_n + (1-a)x_{n-1} \tag{4}$$

where $a = a_0$ and $(1-a) = a_1$ are the filter coefficients from (2). For $a \in (0,1)$ this filter has a smoothing or lowpass characteristic. Henceforth this system will simply be refered to as "the filtered logistic map". For $a = 1$, the system reduces to the ordinary logistic map.

Note that the system (3–4) is a 2-D quadratic map, and using any higher order filter would correspondingly make it a higher dimensional map. Even a first order recursive filter with a_0, $b_1 \neq 0$ and all other coefficients set to zero would result in a three-dimensional system. Zeraoulia & Sprott [2010] investigated the twelve parameter family of 2-D quadratic maps, which includes the filtered logistic map as a special case. They provide criteria for finding chaos and hyperchaos in this parameter space; as we will see, the filtered logistic map is capable of hyperchaos in parts of its parameter space.

Despite being a special case of 2-D quadratic maps, it appears that the map (3–4) has not been studied in detail in the literature so far. Nor is there any theory of filtered maps in general, to the best of my knowledge. In the following, the filtered logistic map is investigated with respect to its fixed points, global stability, transients, and chaos.

2. Fixed points

The filtered logistic map is a two parameter system with two-dimensional variables. Over a large region of the (a, r) parameter plane there are stable fixed points, as can be seen in figure 1. Note the almost perfect vertical symmetry around $r = 1$. At $r = 2$, the logistic map has a superstable period one orbit, and as a is varied, two "arms" of period one stretch out horizontally. The shape and length of these two arms depends on initial condition, whereas those at $r = 0$ unconditionally extend to infinity. In the following, we will restrict r to the positive half-plane. For further analysis, we rewrite the filtered logistic map in delayless form as follows:

$$x_{n+1} = ar(x_n - x_n^2) + y_n \tag{5}$$
$$y_{n+1} = (1-a)r(x_n - x_n^2) \tag{6}$$

Initial conditions will be chosen from the set $[0,1] \times [0,1]$, even though this set is not guaranteed to map into itself under (5–6), and indeed some attractors do extend outside of this region.

Since the fixed points (x^*, y^*) happen to lie on the diagonal $x = y$, we will simplify the notation by refering to the fixed point (x^*, x^*) as x^*. As in the ordinary logistic map, there are two fixed points which satisfy

$$-rx^2 + (r-1)x = 0 \tag{7}$$

which gives

$$x^*_{0,r} = \{0;\ \frac{r-1}{r}\}. \tag{8}$$

The stability of x^* is given by the magnitude of the eigenvalues λ_1 and λ_2 of the Jacobian

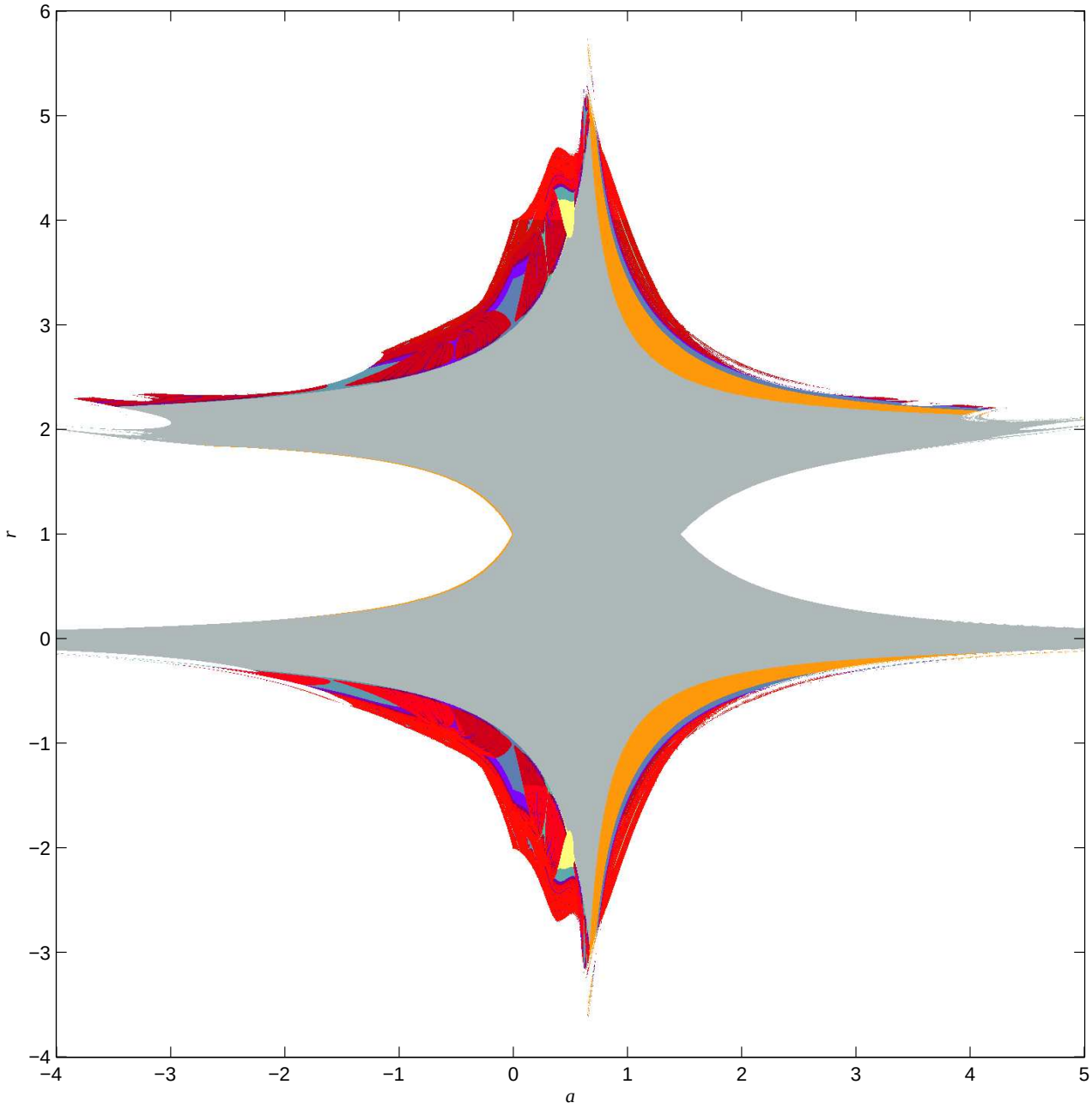

Fig. 1. Bifurcation plot of the filtered logistic map. White is unstable, red is chaotic, grey is period one. The initial condition was $(0.48, 0.52)$, and the plot was made after the first 500 iterations of the map.

$$J = \begin{bmatrix} ar(1-2x) & 1 \\ r(1-a)(1-2x) & 0 \end{bmatrix} \tag{9}$$

evaluated at the fixed points. Thus, we solve $\det(J - \lambda I) = 0$, that is,

$$\lambda^2 - ar(1-2x)\lambda - r(1-a)(1-2x) = 0 \tag{10}$$

which gives

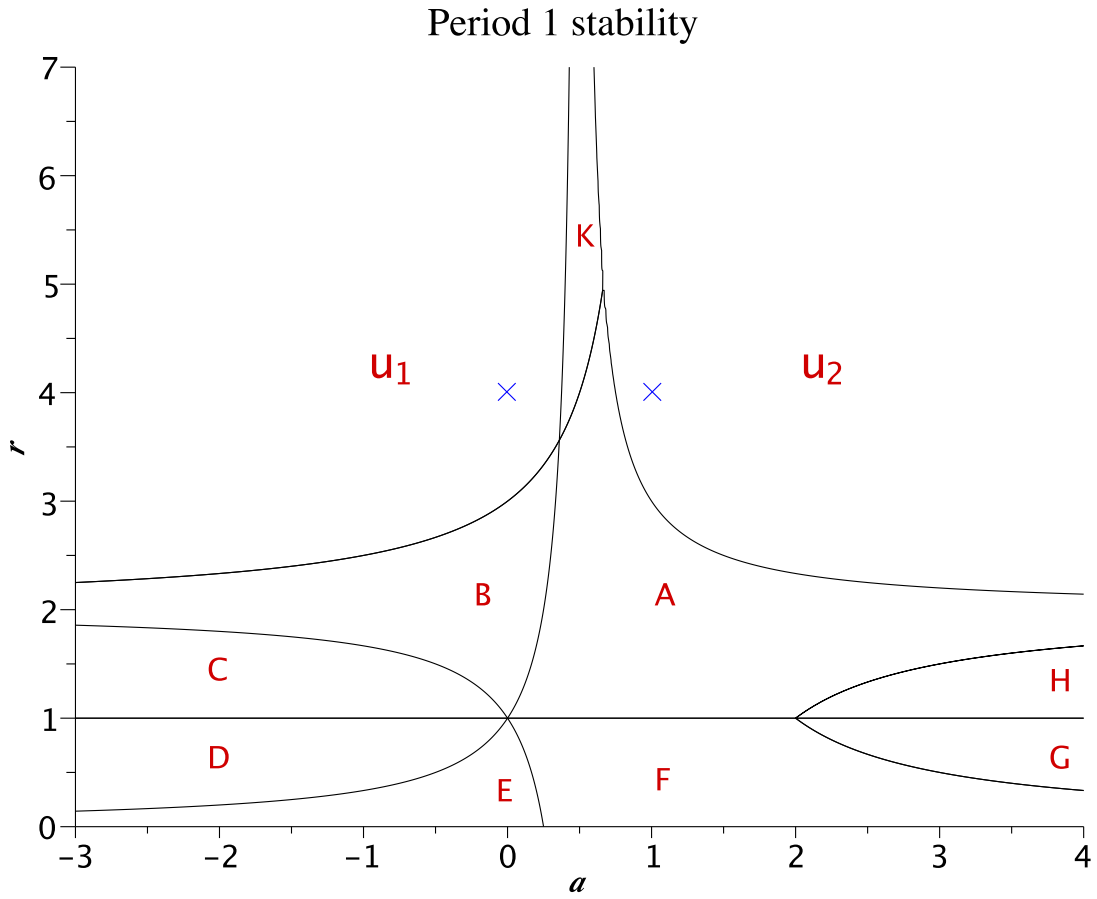

Fig. 2. Stability diagram of period 1 solutions. The curves show the boundaries where $|\lambda| = 1$ for either or both fixed points. The two blue crosses mark the points $(0, 4)$ and $(1, 4)$.

$$\lambda_{1,2} = \frac{1}{2}ar(1-2x) \pm \sqrt{\left(\frac{ar(1-2x)}{2}\right)^2 + r(1-a)(1-2x)}. \tag{11}$$

Inserting the fixed points into (11), we get for $x^* = 0$

$$\lambda_{1,2} = \frac{1}{2}ar \pm \sqrt{\left(\frac{ar}{2}\right)^2 + r(1-a)} \tag{12}$$

and for the fixed point $x^* = (r-1)/r$:

$$\lambda_{1,2} = \frac{1}{2}a(2-r) \pm \sqrt{\left(\frac{a(2-r)}{2}\right)^2 + (r-2)(a-1)}. \tag{13}$$

These fixed points are stable if $|\lambda| < 1$ for both eigenvalues, and a saddle point if $|\lambda_1| < 1 < |\lambda_2|$, and otherwise unstable.

Figure 2 shows the stabilities of period one solutions. The fixed point x_0 is stable in E and F; a saddle point in regions D, A, H, u_2, and K; and it is unstable in regions B, C, G, and u_1. For x_r, its two stable regions are A and B; it is a saddle point in C, F, G and u_2; and unstable in the remaining regions.

The two blue crosses in the unstable u-regions lie at the border of global instability; the system restricted to the line between these two points will be analysed more closely in section 4. The regions C, D, G, H are unstable for almost all initial conditions.

3. Heuristic stability analysis

Let us first consider the system (3–4) as two decoupled systems. Then we recombine them and derive a heuristic stability criterion. To this end, we will study the isolated filter part in the frequency domain, because the magnitude of the frequency response reveals how much gain the filter introduces.

The logistic map is stable for $0 < r < 4$, and attains its maximum $r/4$ at $x = 0.5$. It can be shown that for $r = 4$, there exist initial conditions $x_0, y_0 \in [0, 1]$ such that the system becomes unstable only for $a < 0$ or $a > 1$. Hence at least a rectangular domain $(a, r) \in [0, 1] \times [0, 4]$ can be identified where the system is guaranteed to be stable. But better stability criteria can be found.

For the filter, we use it as written in eq. 4, and treat it as if it were nonrecursive. Its z-transform is $H(z) = a + (1 - a)z^{-1}$ and the frequency response is

$$H(e^{i\omega}) = a + (1 - a)e^{-i\omega}. \tag{14}$$

Note the two limiting cases $a = 1$ corresponding to the ordinary logistic map, and $a = 0$ which is a delayed logistic map; both are trivial allpass filters. For intermediate values, the filter can be seen as a simple interpolation from no delay to a unit delay.

The magnitude of the filter's frequency response is

$$|H(e^{i\omega})| = \sqrt{a^2 + (1 - a)^2 + 2(a - a^2)\cos\omega}. \tag{15}$$

Figure 3 shows the magnitude of the filter's frequency response for several values of a. Note that the curves for $a = 0$ and $a = 1$ coincide; and so do the curves for $a = 2$ and $a = -1$, etc. In other words, there is a symmetry around $a = 0.5$. Hence it is not entirely unreasonable to expect some symmetry on the a-axis of the filtered logistic map too. Indeed, the bifurcation plot (figure 1) shows an imperfect, skewed kind of symmetry along the a-axis.

Since the frequency response magnitude (15) is a monotonic function, its maximum must be either at $\omega = 0$ or at $\omega = \pi$. In the range $a \in (0, 1)$ the filter is lowpass, and at $\omega = 0$, eq. (15) acquires its maximum $H(e^{i\omega})|_{\omega=0} = 1$. Outside this range, i.e. for $|a - \frac{1}{2}| > \frac{1}{2}$, the filter is highpass. Evaluating the gain at the Nyquist frequency $\omega = \pi$ and combining these two cases, we get the following formula for maximum gain:

$$G(a) = \begin{cases} 1 & \text{if } a \in [0, 1] \\ \sqrt{4(a^2 - a) + 1} & \text{if } a \notin [0, 1] \end{cases} \tag{16}$$

A theoretical global stability region is given by the condition $G(a)r/4 < 1$. In particular, for $r < 4$, there will be some $a \notin [0, 1]$ still fulfilling the stability condition. This stability region is marked in figure 4. Also, for $a \in (0, 1)$ there are some $r > 4$ for which the system is stable (see figure 2), at least for some initial conditions. The filter gain formula does not predict these attractors, which slightly overshoot the (wrongly) assumed limits of stability $x \in [0, 1]$, as can be seen in the attractor plots (figure 5).

Setting $a = 0.5$, the filter has a zero at the Nyquist frequency, in other words it suppresses period two oscillations. By continuity of the filter transfer function under small variations of coefficient, one should expect that period two cannot exist close to $a = 0.5$ in the filtered logistic map. This is in agreement with what can be seen in figure 4.

There is another approach to stability estimation if we think of the filter as recursive, and for simplicity ignore the nonlinearity of the logistic map. Using as input the initial condition $x_n = x_0\delta_n$ (with the Dirac delta function), the filter may be written as

$$y_n = x_n + ay_{n-1} + (1 - a)y_{n-2} \tag{17}$$

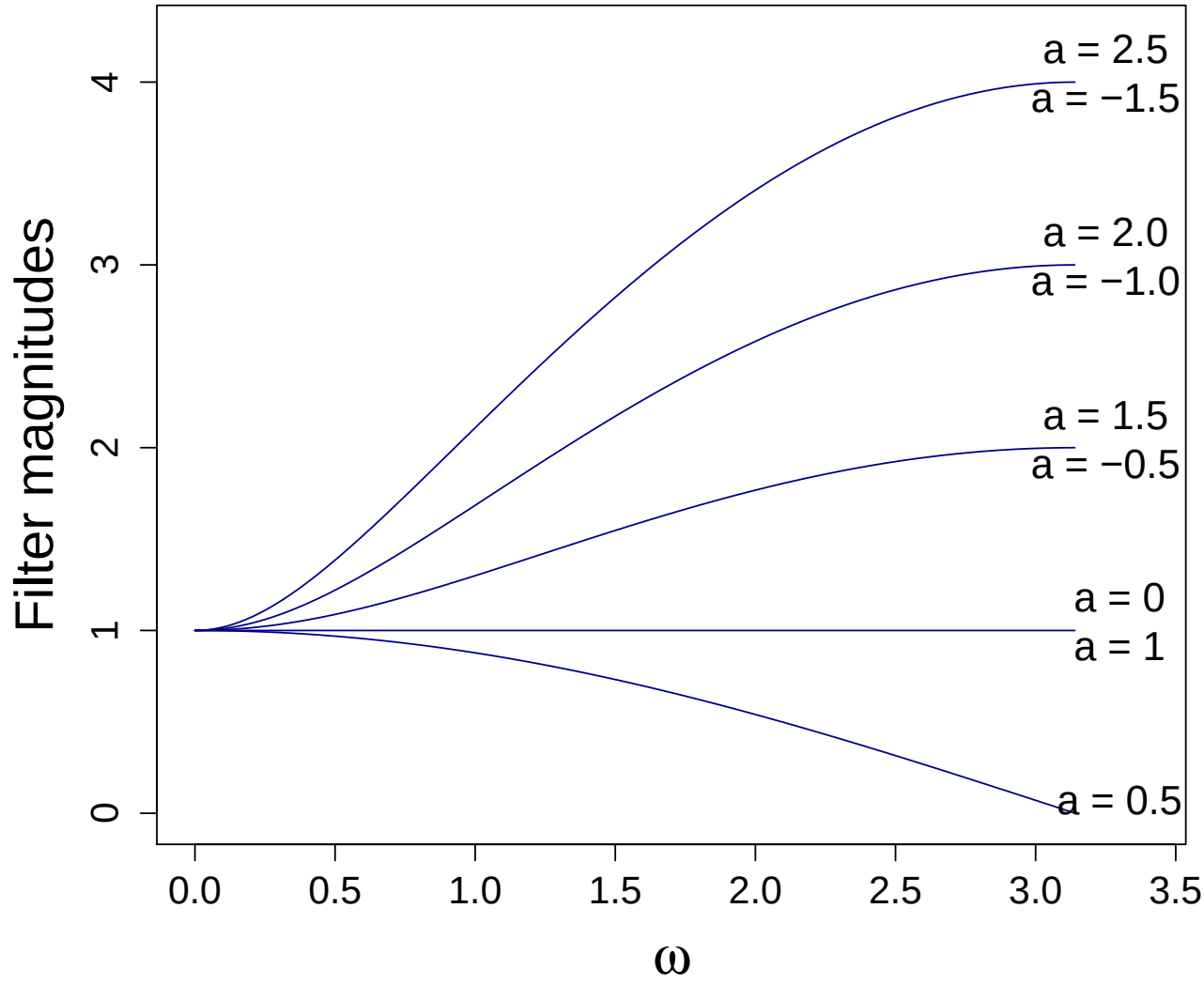

Fig. 3. Frequency response $|H(e^{i\omega})|$ of the filter. Note that $a = 0$ and $a = 1$ results in identical curves; likewise for $a = 2$ and $a = -1$, and so on.

with z-transform $H(z) = 1/(1 - az^{-1} - (1 - a)z^{-2})$. For $a = 1$ the filter has a pole at $z = 1$ (resonance at DC), while for $a = 0$ there are poles at $z = \pm 1$ (additional resonance at $\omega = \pi$).

4. The lines $r = 4$, and $a = 0$

By fixing either a or r, we get a one-parameter system. Let us consider first the case $r = 4$. For $r = 4$ and $0 < a < 1$, the fixed point $x^* = 0$ is a saddle node for $a > 3/8$ and becomes unstable for $a < 3/8$. The other fixed point, $x^* = 3/4$, undergoes a bifurcation at the critical point $a_c = 1/2$; for $a > a_c$ it is a saddle node, and for $a < a_c$ it becomes unstable. This can be seen also from the bifurcation plot (top of figure 6), where the attractor of an initial condition close to the fixed point $(3/4 + \epsilon, 3/4 - \epsilon)$ with $\epsilon = 0.0001$ is shown in red. The blue-colored points stem from the initial condition $(0.5, 0.5)$, which has also been used for the spectrum below. The spectral bifurcation plot reveals what we might call a spectral bifurcation (quasi-periodicity) as a decreases beyond the period three window. For $a < 0.3$ there are intervals where

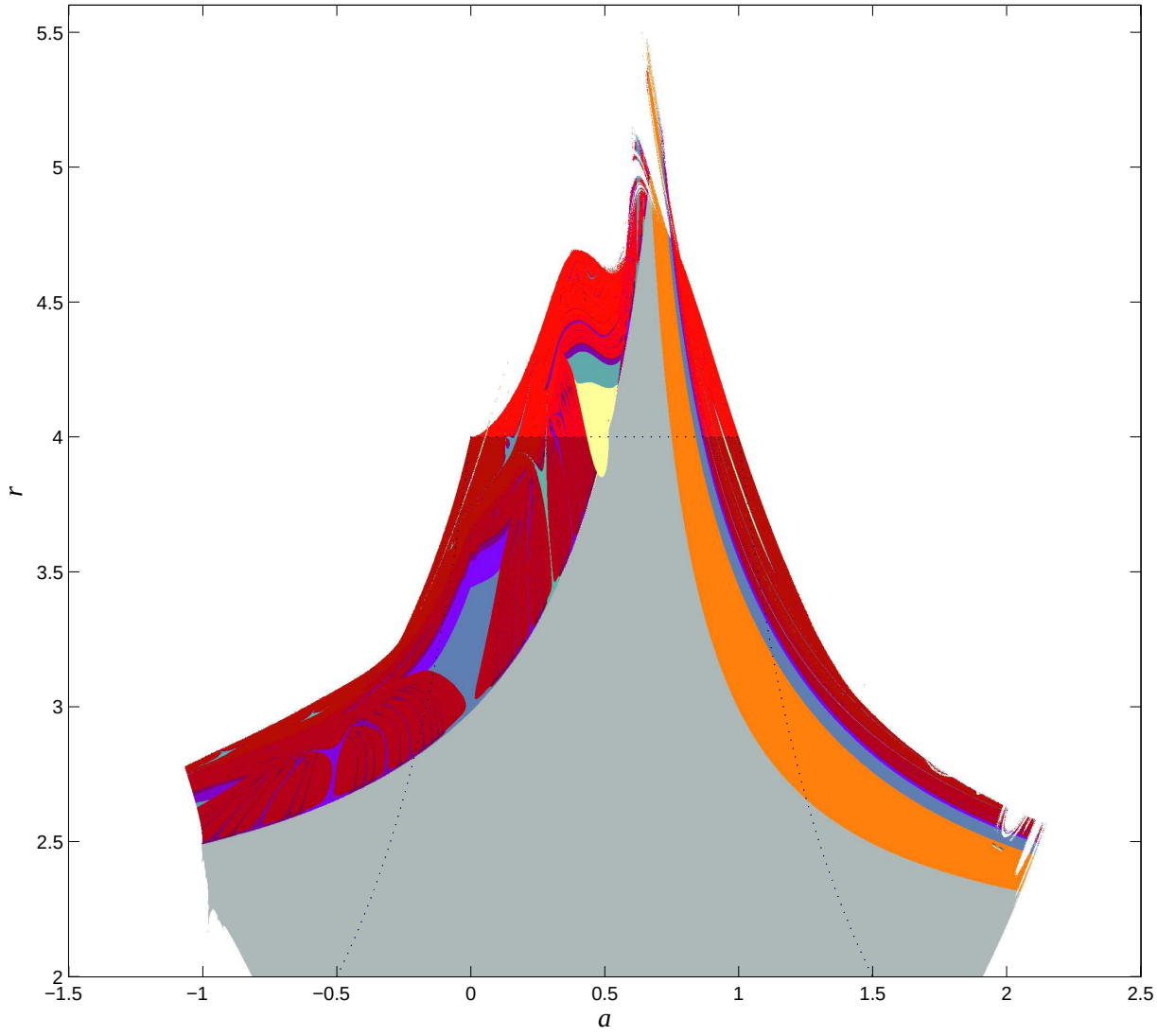

Fig. 4. Bifurcation plot with initial condition $(0.6, 0.4)$. Stability according to $rG(a)/4 < 1$ is below the black dotted curve. The color map is as follows: Gray, period one; orange, period two; light yellow, period three; higher periods in various blue and green shades; dark and bright red, chaos; white is unstable.

both Lyapunov exponents are positive, so the map is hyperchaotic in a region close to $(0, 4)$ in the (a, r) plane (see bottom of figure 6).

Note the similarity with the ordinary logistic map for $a > 0.6$ (from period one): there is the same period doubling cascade, band merging, and period 3 window that is familiar from the logistic map. This is obvious from looking at figure 4, where it can be seen that regions of period 2, 4, etc, and the period three window cuts diagonally across the plane.

The left half of the strip $r = 4$ in figure 6 is quite different, with a window in the interval $a \in (0.1168, 0.1743)$ where period five is prominent, but interspersed with intervals of mostly odd multiples of period five; in particular, there are several 'bubbles' of period 15. In the interval $a \in (0.304, 0.331)$ there is a period ten window, also shown in figure 7. A period ten attractor (the ten disconnected points) is coexisting with an attractor with a closed contour; the small circular shapes in the third plot from left is typical of a Neimark-Sacker bifurcation.

Setting $a = 0$ results in a (trivially) delayed logistic map. Its difference equation reduces to

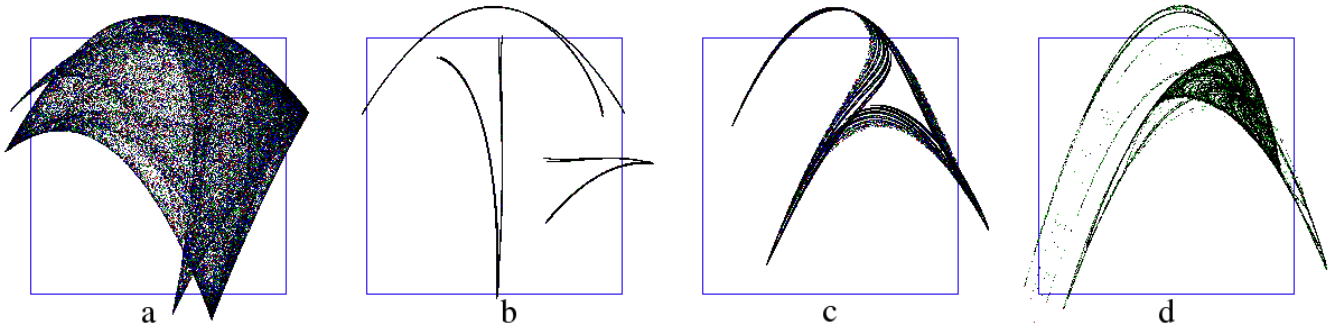

Fig. 5. Attractors above $r = 4$, near instability. Parameter locations and Lyapunov exponents (LE) from left to right: a) $(a, r) = (0.25, 4.36), LE_1 = 0.2269, LE_2 = 0.1186$; b) $(0.35, 4.5), LE_1 = 0.2127, LE_2 = -0.3867$; c) $(0.50, 4.5), LE_1 = 0.2189, LE_2 = -0.3237$; d) $(0.57, 4.64), LE_1 = 0.13, LE_2 = -0.26$, where the Lyapunov exponents only converge for some initial conditions. The Lyapunov exponents have been calculated after an initial transient of 1000 iterations and running the map for 25000 iterations. The boxes mark the regions $(x, y) \in [0, 1] \times [0, 1]$.

$$x_n = r x_{n-2}(1 - x_{n-2}), \tag{18}$$

which is just an interleaved sequence of two independent logistic maps with identical parameter, but possibly differing initial conditions. Hence, there cannot exist any odd periods (except for period one) in the orbits of x_n. The bifurcation diagram at $a = 0$ looks almost identical to that of the ordinary logistic map. However, the difference is that all period lengths will be doubled in the delayed map. The only exception is the period one orbit, which is only possible if the initial conditions in (18) are identical, i.e. $x_0 = x_1$.

As the parameter point $(a, r) = (0, 4)$ is approached from $a > 0$, or from $r < 4$, the attractor fills more and more of the box $[0, 1] \times [0, 1]$. At the parameter location $(0, 4)$ there are three different attractors, as shown leftmost in figure 8; one of them consists of the parabola $y = 4x(1 - x)$ together with the line $y = x$ (in red), another is a cross (green), and finally there is the area filling attractor. The two Lyapunov exponents (LE) are equal along the line $a = 0$, which is exactly what one would expect from two decoupled but identical systems. At $r = 4$ they are $LE_1 = LE_2 = 0.34654$, which can be compared to the single Lyapunov exponent $LE = \log(2) = 0.6931$ of the logistic map at $r = 4$. Since the two logistic maps at $a = 0$ may be thought of as running at half rate compared to the one at $a = 1$, it is to be expected that their Lyapunov exponents have exactly half the magnitude of those at the ordinary logistic map.

5. Transients

For a stable linear filter, the length of its impulse response may be defined as the time it takes the signal to decay to a sufficiently small value $0 < |\epsilon| \ll 1$. In the case of maps, the transient length may be similarly defined as the time it takes before an orbit comes sufficiently close to an attractor. Clearly this will depend on initial conditions; starting on the attractor results in no transient at all. But it also depends on ϵ and the parameters of the map.

If the attractor is periodic or a fixed point, the transient length τ is given by the smallest n such that the distance from the orbit x_n to the orbit on the attractor ρ_n is below some minimum ϵ,

$$\tau = \inf\{n : |x_n - \rho_n| < \epsilon\}, \tag{19}$$

provided the two orbits are aligned in time so as to minimize this difference.

For an estimate of transient length, first a reference orbit ρ_n is generated from the initial condition $(0.5, 0.5)$, then the test orbit is compared against the reference. The measured transient lengths are plotted for various initial conditions in figure 9. Transients become very long near bifurcations, but there are also some other regions with quite long transients. The maximum number of iterations was set to 500,000; the

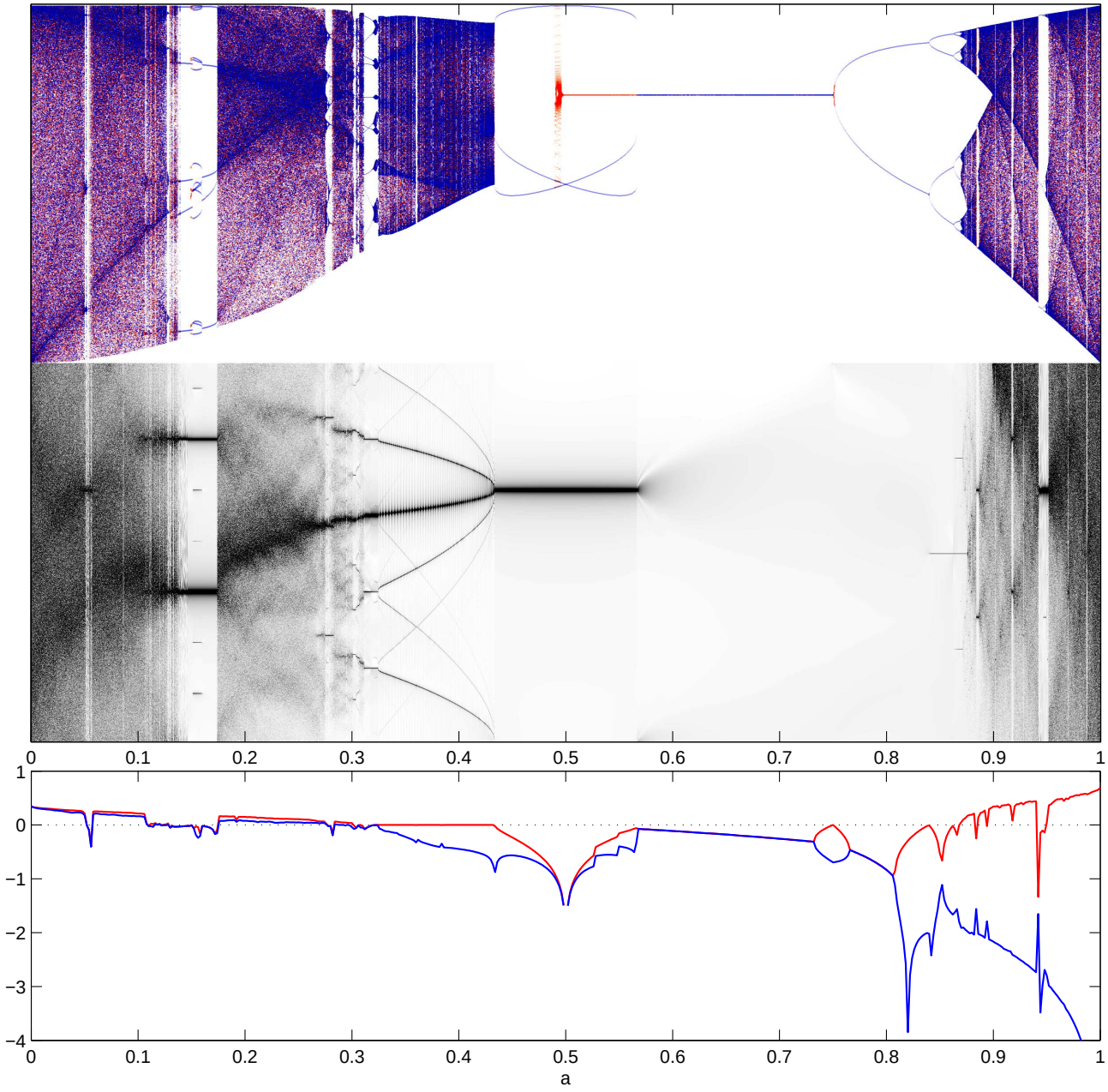

Fig. 6. From top to bottom: Bifurcation and spectral bifurcation plot, and Lyapunov exponents at $r = 4$. Lyapunov exponents are obtained after an initial transient of 1000 iterations, and calculated from 25000 iterations of the map.

orbits close to bifurcations do not converge to within $\epsilon = 10^{-15}$ even after so many iterations. Instead, $\epsilon = 10^{-12}$ was used in figure 9. Note however that about 2^{10} iterations is sufficient for convergence at a vast majority of parameter values. A caveat must be added: there are points in the parameter space with at least two coexisting attractors; care must be taken when measuring transients at these points.

This method does not apply to chaotic orbits, at least not without some modification. The duration of chaotic transients can be estimated in the case of boundary crises and interior crises [Grebogi *et al.*, 1983].

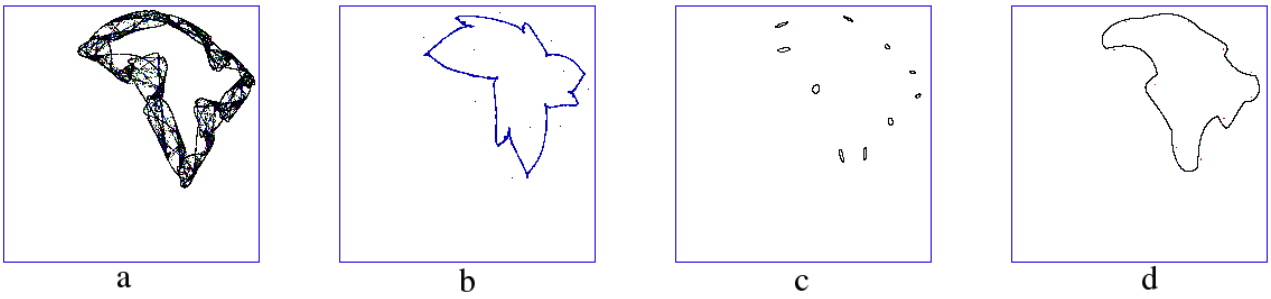

Fig. 7. Bifurcations around the period 10 window at $r = 4$. Lyapunov exponents from left to right: a) $a = 0.3, LE_1 = 0.0349, LE_2 = -0.0414$; b) $a = 0.305, LE_1 = 0.0076, LE_2 = -0.0132$; c) $a = 0.322, LE_1 \approx 0.0, LE_2 = -0.0042$; d) $a = 0.325, LE_1 \approx 0.0, LE_2 = -0.0653$.

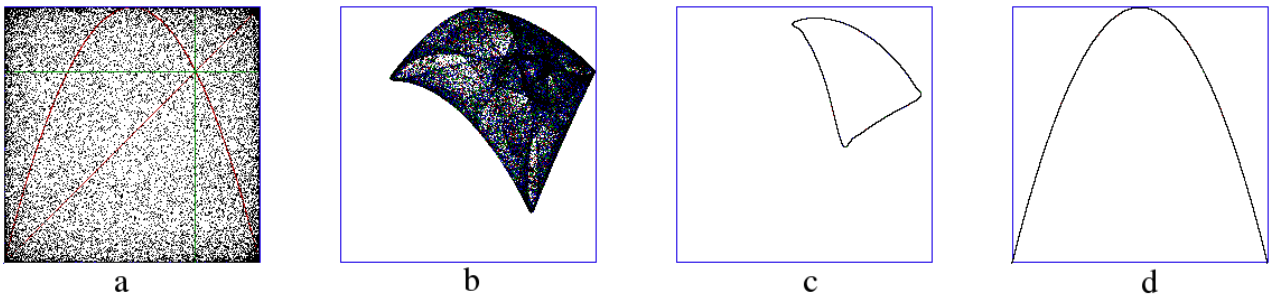

Fig. 8. Some attractors at $r = 4$ and their Lyapunov spectrum, from left to right: a) $a = 0.0, LE_1 = LE_2 = 0.3465$, corresponding to two interleaved logistic maps; b) $a = 0.25, LE_1 = 0.1061, LE_2 = 0.0463$; c) $a = 0.4, LE_1 \approx 0.0, LE_2 = -0.4444$, with quasi-periodic orbits; d) $a = 1.0, LE = 0.6931$, the ordinary logistic map.

6. Conclusion

The logistic map filtered with a first order non-recursive filter is a quadratic 2-D map, and also the simplest case of a filtered map with a quadratic nonlinearity. The filter has a stabilizing effect in the region where it has a lowpass characteristic. In particular, the period 1 solutions remain stable for some values of a even for $r > 4$, which contrasts with the boundary crisis that occurs in the logistic map at $r = 4$. At $a = 0.5$ the filter blocks period two oscillations completely. With higher order filters, one may introduce zeros at other frequencies in the filter's frequency response, so that oscillations of arbitrary periods may be blocked.

The filter coefficient may also be seen as a parameter regulating the coupling between two logistic maps, with hyperchaos resulting when the coupling is weak. Chaos suppression can be acheived by inserting a lowpass filter in the feedback path.

Filters and delays in the feedback loop of maps are important elements in musical sound synthesis by physical modeling. The filtered logistic map would need an extra delay component in the filter in order to be useful as a sound synthesis algorithm.

Many open questions concerning filtered maps in general remain to be investigated: What kinds of filters are amenable to produce or reduce chaos; what maps can be used to produce chaos in combination with a given filter? We have looked at transient lengths of some periodic orbits, but it would be useful to have a unified framework that allows comparisons of transient lengths regardless of whether the orbit is periodic, chaotic, quasi-periodic, or eventually unbounded.

Acknowledgments

The author would like to thank Rolf Inge Godøy and Sverre Holm at the University of Oslo, and the three

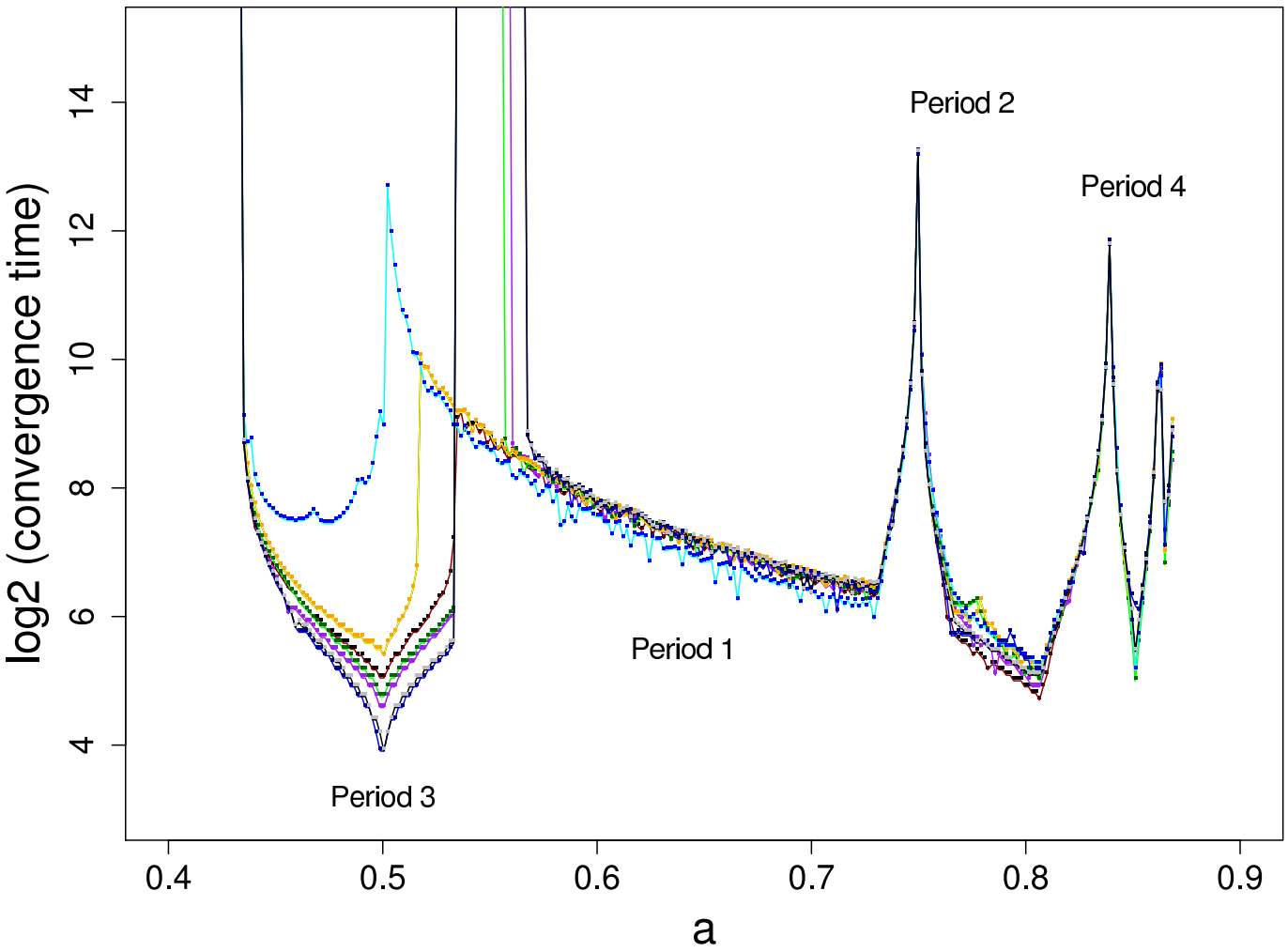

Fig. 9. Transient length (logarithm of convergence time) at $r = 4$ for various initial conditions. The light blue curve was started from the initial condition $(0.74, 0.76)$, that is, close to the fixed point.

anonymous reviewers for all their useful comments.

References

Bernardi, A., Bugna, G. & De Poli, G. [1997] "Musical signal analysis with chaos," *Musical Signal Processing*, eds. Roads, C., Pope, S., Piccialli, G. & De Poli, G. (Swets and Zeitlinger), pp. 187–220.

Buchner, T. & Żebrowski, J. [2000] "Logistic map with a delayed feedback: Stability of a discrete time-delay control of chaos," *Physical Review E* **63**.

Chua, L. & Lin, T. [1988] "Chaos in digital filters," *IEEE Transactions on Circuits and Systems* **35**, 648–658.

Grebogi, C., Ott, E. & Yorke, J. [1983] "Crises, sudden changes in chaotic attractors, and transient chaos," *Physica D* **7**, 181–200.

Holopainen, R. [2010] "Self-organised sounds with a tremolo oscillator," *Proc. of the 13th Int. Conference on Digital Audio Effects (DAFx-10)* (Graz, Austria), pp. 412–418.

Rodet, X. [1993] "Models of musical instruments from Chua's circuit with time delay," *IEEE Transactions on Circuits and Systems–II: Analog and Digital Signal Processing* **40**, 696–701.

Rodet, X. & Vergez, C. [1999] "Nonlinear dynamics in physical models: From basic models to true musical-instrument models," *Computer Music Journal* **23**, 35–49.

Zeraoulia, E. & Sprott, J. C. [2010] *2-D Quadratic Maps and 3-D ODE Systems*, Nonlinear Science, Series A, Vol. 73 (World Scientific, Singapore).